Lawrence Berkeley National Laboratory

LBL Publications

Title

Cool Roofs in Guangzhou, China: Outdoor Air Temperature Reductions during Heat Waves and Typical Summer Conditions

Permalink

https://escholarship.org/uc/item/5h32p3sk

Journal

Environmental Science and Technology, 49(24)

ISSN

0013-936X

Authors

Cao, Meichun

Rosado, Pablo

Lin, Zhaohui

et al.

Publication Date

2015-12-15

DOI

10.1021/acs.est.5b04886

Peer reviewed

eScholarship.org Powered by the California Digital Library
University of California

Cool Roofs in Guangzhou, China: Outdoor Air Temperature Reductions During Heat Waves and Typical Summer Conditions

Authors:

Meichun Cao[1], Pablo Rosado, Zhaohui Lin[1], Ronnen Levinson, Dev Millstein

[1]International Center for Climate and Environment Sciences, Institute of Atmospheric Physics, Chinese Academy of Sciences, Beijing 100029, China

Energy Analysis and Environmental Impacts Division
Lawrence Berkeley National Laboratory

December 2015

This is a pre-print version of an article published in *Environmental Science and Technology*.

DOI: http://doi.org/10.1021/acs.est.5b04886

This work was supported by the US-China Clean Energy Research Center – Building Energy Efficiency and support from the Strategic Priority Research Program of the Chinese Academy of Sciences (XDA05110200) and the National Natural Science Foundation of China (Grant No. 41305093). The study was further supported by the Assistant Secretary for Energy Efficiency and Renewable Energy, Office of Building Technology, State, and Community Programs, of the U.S. Department of Energy under Contract No. DE-AC02-05CH11231. This research used resources of the National Energy Research Scientific Computing Center, a DOE Office of Science User Facility supported by the Office of Science of the U.S. Department of Energy under Contract No. DE-AC02-05CH11231. under Lawrence Berkeley National Laboratory Contract No. DE-AC02-05CH11231.

DISCLAIMER

This document was prepared as an account of work sponsored by the United States Government. While this document is believed to contain correct information, neither the United States Government nor any agency thereof, nor The Regents of the University of California, nor any of their employees, makes any warranty, express or implied, or assumes any legal responsibility for the accuracy, completeness, or usefulness of any information, apparatus, product, or process disclosed, or represents that its use would not infringe privately owned rights. Reference herein to any specific commercial product, process, or service by its trade name, trademark, manufacturer, or otherwise, does not necessarily constitute or imply its endorsement, recommendation, or favoring by the United States Government or any agency thereof, or The Regents of the University of California. The views and opinions of authors expressed herein do not necessarily state or reflect those of the United States Government or any agency thereof, or The Regents of the University of California.

Ernest Orlando Lawrence Berkeley National Laboratory is an equal opportunity employer.

COPYRIGHT NOTICE

This manuscript has been authored by an author at Lawrence Berkeley National Laboratory under Contract No. DE-AC02-05CH11231 with the U.S. Department of Energy. The U.S. Government retains, and the publisher, by accepting the article for publication, acknowledges, that the U.S. Government retains a non-exclusive, paid-up, irrevocable, worldwide license to publish or reproduce the published form of this manuscript, or allow others to do so, for U.S. Government purposes.

Cool Roofs in Guangzhou, China: Outdoor Air Temperature Reductions During Heat Waves and Typical Summer Conditions

Meichun Cao[1], Pablo Rosado[2], Zhaohui Lin[1], Ronnen Levinson[2], and Dev Millstein[2]*

*Corresponding Author: Dev Millstein, dmillstein@lbl.gov, (510) 485-4556.

Abstract

In this paper we simulate temperature reductions during heat-wave events and during typical summer conditions from the installation of highly reflective "cool" roofs in the Chinese megacity, Guangzhou. We simulate temperature reductions during six of the strongest historical heat-waves events over the past decade, finding average urban midday temperature reductions of 1.2 °C. In comparison, we simulate 25 typical summer weeks between 2004 and 2008, finding average urban midday temperature reductions of 0.8 °C, indicating that air temperature sensitivity to urban albedo in Guangzhou varies strongly based on meteorological conditions. We find that roughly three-fourths of the variance in air temperature reductions across all episodes can be accounted for by a linear regression including only three basic properties related to the meteorological conditions: mean daytime temperatures, humidity, and ventilation to the greater Guangzhou urban area. While these results highlight the potential for cool roofs to mitigate peak temperatures during heat waves, the temperature reductions reported here are based on the upper bound case where all roofs are modified to be more reflective (but does not include changes to road or wall reflectivity).

[1] International Center for Climate and Environment Sciences, Institute of Atmospheric Physics, Chinese Academy of Sciences, Beijing 100029, China

[2] Heat Island Group, Lawrence Berkeley National Laboratory, Berkeley, CA, 94720, USA

TOC/Abstract Art.

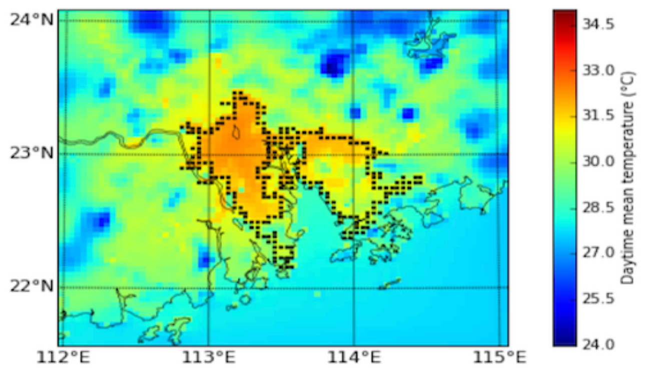

1 Introduction

Increasing the solar reflectance (albedo) of roofs can cool buildings, reducing air conditioning use,[1,2,3,4] and lower city-wide outdoor air temperatures.[5,6,7,8,9,10] From a global perspective, increasing the average albedo of existing urban areas (roughly 2% of total land area)[11] is studied as a potential strategy to partially counteract climate change by reducing the net radiation absorbed by the Earth.[12,13,14,15,16] Furthermore, meteorological modeling of North America indicates that urban expansion alone, in the absence of adaptations to reduce heat gain, may cause regional temperature increases that are similar in magnitude to greenhouse gas driven warming.[17] To encourage adoption of high-albedo ("cool") roofs, a number of state and local governments around the world are considering or already mandate the use of cool roofing materials for certain building types.[18,19,20] Since 2010 the governments of the United States and China have been coordinating building energy efficiency research efforts within the U.S.-China Clean Energy Research Center Building Energy Efficiency (CERC-BEE) Consortium.[21] As a product of this joint effort, we explore the potential for reflective roofs to cool Guangzhou, one of the most populous urban areas in southern China. Related work from CERC-BEE investigated the building energy use implications of switching to cool roofs across various regions in China.[20]

In China, mitigation of urban heat islands could benefit the large population living in cities with hot summers. Despite this potential benefit, only a limited number of studies have simulated air temperature reductions due to the deployment of cool roofs in cities in China. For example Wang et al22 and Ma et al23 simulated the potential for cool roofs to mitigate heat-wave events in Beijing. Li et al24 explored synergies between urban heat islands and heat waves in Beijing and explicitly recommended studying white and green roofs as a mitigation strategy.

In general, heat waves can pose significant public health problems.25 Additionally, electricity grids are typically under the most stress during heat waves.26,27 In southern China Yang et al.28 found that a 2005 heat wave had a significant impact on mortality rates in Guangzhou. In summer, southern China is located between the Western Pacific subtropical high and the Inter-Tropical Convergence Zone, and the climate is often influenced by tropical weather systems such as typhoons. High temperature events in this region are primarily caused by the adiabatic compression heating of the downdraft in west of the typhoon periphery and are occasionally caused from subtropical high subsidence airflow.29

In the U.S. and Europe many studies have evaluated potential air temperature reductions as a result of cool roof deployment by modeling a single brief (2 – 4 day) episode, often an unusually hot episode. A logical follow up question: Are the temperature reductions found during a single hot episode representative of temperature reductions that would be found over a whole season? Taha30 simulated the effects of increased albedo across a range of meteorological conditions associated with varying ozone conditions in central and southern California, but did not find strong correlation between daily maximum temperatures and simulated temperature reductions. Mihalakakou et al.31, however, found that synoptic conditions strongly determined the heat island intensity in Athens, Greece, and Zhao et al.32 found that the intensity of urban warming depends on local background climate in cities across the United States.

This paper breaks new ground on two fronts. It is one of a limited number of studies to evaluate potential air temperature reductions from cool roof deployment in Chinese cities. It is also the first study to directly compare the potential air temperature reductions during historic Southern China heat-wave events to the potential air temperature reductions during typical summer time periods. To make this comparison we model six of the strongest historical heat waves in Southern China over the past decade, as well as 25 randomly sampled summer weeks between 2004 and 2008.

Finally, the scope of this paper is limited to modeling the meteorological effects of cool roofs. The combination of air temperature reductions and reduced boundary layer height, commonly found when simulating cool roof adoption, can have either positive or negative impacts on air quality depending on the local meteorological conditions and the relative concentrations of air pollutants.[33] We leave for future research the necessary emission and air quality modeling required to accurately assess the potential air quality impacts of cool roofs.

2 Methods

2.1 Modeling setup

Meteorological simulations were performed using the Weather Research and Forecasting model, WRF version 3.6.[34] A triple-nested domain was used (Fig. 1), with grid resolutions of 36-, 12-, and 4-km. The outermost domain, centered at 23.17^{o}N and 113.33^{o}E, with horizontal dimensions of 2520 km × 2520 km and individual grid cells with 36 km horizontal resolution, encompasses the hot summer and cold winter regions of southern China.[35] The intermediate domain provides a resolution of 12 km and covers an area of 840 km × 840 km. The innermost domain covers a 316 km × 280 km area and resolves the Guangzhou megacity area and the local surrounding hills in high resolution (4 km). Figure 1 shows the ground elevation across the three nested domains, and a close up view of the inner most domains. The vertical grid contains 38 levels from the surface to 50 hPa, of which the lowest 7 levels are below 1 km to show a finer resolution in the planetary boundary layer. Each modeling episode was run with a single day of spin-up time.

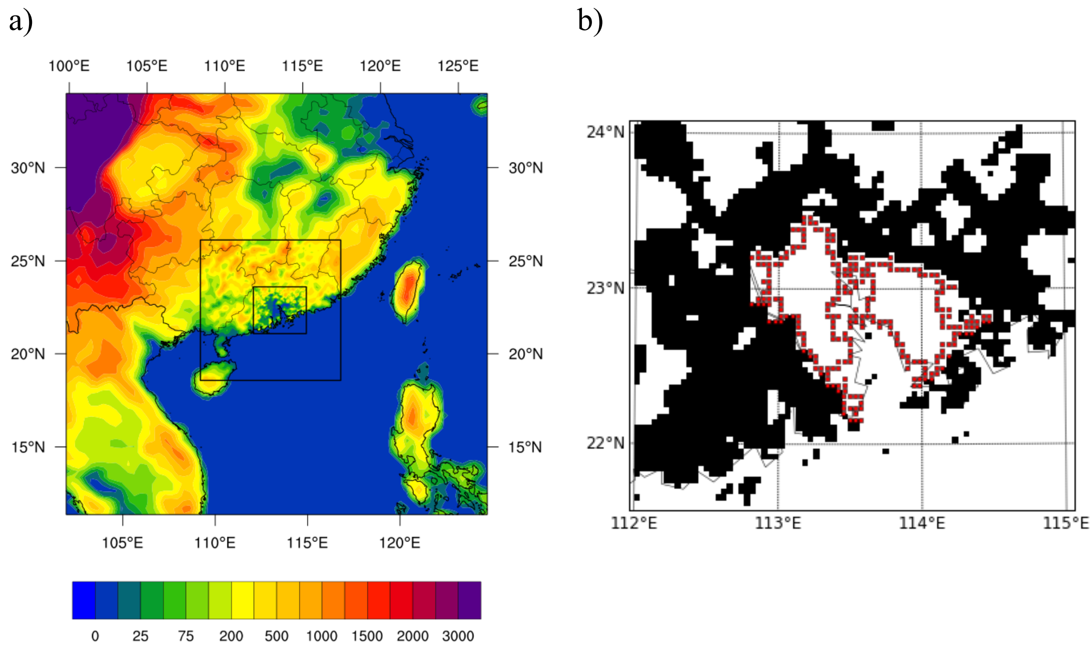

Figure 1. (a) Elevation map showing the two-way triple-nested simulation domains and the terrain height above sea level (m) in each domain: the two rectangles are the intermediate and inner domain, respectively. (b) The inner most modeling domain: the red line bounds the greater Guangzhou urban area, while the portions in black are rural areas with altitudes less than 200 m above the sea level.

Both the initial and the boundary conditions were from the six-hourly National Centers for Environmental Predictions (NCEP) operational Global Final (FNL) Analyses on a $1^{o} \times 1^{o}$ grid. Land use was derived from the Moderate Resolution Imaging Spectroradiometer (MODIS) 20-category land dataset in 2001~2004. Sea surface temperature is updated daily based on the AVHRR product from NOAA.36 Instead of leaf area index (LAI) information from a static table, we use the 12-monthly, 30-second LAI dataset derived from MODIS. We also use the monthly background surface albedo inputs from the Advanced Very High Resolution Radiometer (AVHRR) on a polar orbiting satellite.37

The urban area in and around Guangzhou was represented in WRF using the Noah land surface model coupled with the single-layer Urban Canopy Model (UCM)38 and the modified Zilitinkevich relationship for thermal roughness length parameterization39. Road, roof and building dimensions in U.S. and European cities are smaller than those in Beijing40,22, and we employed the high-intensity residential parameterizations reported by Wang et al.22 to characterize the urban dimensions in the UCM. Selected parameters used in the UCM are shown in Table 1. We note that due to a lack of detailed urban morphology data we characterized all urban area as the high-intensity residential category within the UCM model. For non-urban cells we use the Noah mosaic method to represent the land surface heterogeneity, which allows three tiles to coexist within a grid cell.41 Surface layer physics was modeled with the MM5 similarity surface layer scheme42 and the planetary boundary layer was modeled with the Yonsei Unversity (YSU) scheme43. Atmospheric radiative transfer (both shortwave and longwave) was modeled with the Rapid Radiative Transfer Model for GCMs (RRTMG).44 Ozone and aerosol properties relative to radiative transfer were based on the climatological values that vary spatially and temporally (monthly). The cloud microphysics processes were modeled with the Lin et al. scheme45. The Grell-Freitas cumulus parameterization46 was employed in the two outer domains; no cumulus parameterization was used in the inner most domain.

Table 1. Selected parameter values for the single-layer UCM.

Parameter	Value	Unit
Urban anthropogenic heating	50	$W\ m^{-2}$
Road width	15	m
Roof width	20	m
Fraction Building or Road	0.8	none
Building height	13	m
Standard deviation of building height	3	m
Heat capacity of roof	1.2×10^6	$J\ m^{-3}\ K^{-1}$
Heat capacity of building walls	1.2×10^6	$J\ m^{-3}\ K^{-1}$
Heat capacity of ground	1.5×10^6	$J\ m^{-3}\ K^{-1}$
Thermal conductivity of roof	0.4	$W\ m^{-1}\ K^{-1}$
Thermal conductivity of building walls	1.0	$W\ m^{-1}\ K^{-1}$
Thermal conductivity of ground	0.8	$W\ m^{-1}\ K^{-1}$
Albedo of roof	0.12	none
Albedo of building walls	0.12	none
Albedo of ground	0.12	none

2.2 Experimental design

We designed our experiment to explore two questions: (1) what are the average summertime meteorological effects of adopting cool roofs across Guangzhou; and (2) how do those effects differ during summer heat-wave events? We modeled 31 episodes, each four to six days long, in two scenarios: a ‘control’ case with roof albedo equal to 0.12, and a ‘cool’ case with roof albedo equal to 0.55. The cool case albedo corresponds to the aged albedo of currently available white roofing products.47 Although some field applied roofing products are installed with initial albedo much higher than 0.55, Sleiman et al48 show that, in hot and humid or polluted regions in the U.S., the aging process lowers albedo to about 0.6. Similar experimental results are not yet available in China.

Building wall and pavement albedo were held constant at 0.12 across both scenarios. The average albedo across the greater Guangzhou urban area (including all horizontal surfaces, not just roofs) was 0.12 in the control case and 0.30 in the cool case. We believe this represents a realistic upper bound to potential albedo enhancement from cool roofs in Guangzhou.

Out of 31 total episodes, six episodes, referred to hereafter as ‘heat-wave’ episodes, were extreme heat-wave events during the last decade (from 2001 to 2010). Heat waves in Guangzhou are commonly associated with one of two types of atmospheric circulation patters, namely Subtropical high-Typhoon-dominated (ST) and Subtropical high (S)-dominated.49 We have not attempted to compile a complete database of heat wave events and have simply chosen to simulate a sample of major heat waves. We chose three episodes of each type that have been identified and studied in previous published research50,51,52,53, and where each episode met the most simple heat wave warning criteria designed by the China Meteorological Administration of three consecutive days with temperatures above 35° C. For ST-dominated type, the episodes are 29 June - 3 July 2004, 14-18 July 2005, and 11-15 July 2007. For S-dominated type, the episodes are 21-25 August 2001, 14-18 July 2003, and 1-5 August 2004. The other 25 episodes, referred to hereafter as ‘normal’ episodes, were selected from the summers of 2004-2008 to provide a representative sample of the average effects of cool roofs during summertime. The normal episodes were chosen simply based on a consistent calendar starting day so the episodes did not overlap with any of the 6 historic heat waves. The normal episodes covered the 19th-24th of each month May through September. Those dates cover the hottest period of the year in Guangzhou. Each of the 31 episodes was begun at 00:00 UTC, with the first 24h discarded as spin up.

2.3 Theory and analysis framework

In the results and discussion section, simulated 2-meter air temperature change in the greater Guangzhou urban area is presented as a function of control scenario air temperature (Equation 1); as a function of control scenario air temperature and urban ventilation (Equation 2); and finally as a function of control scenario air temperature, urban ventilation, and humidity (Equation 3). These regressions were developed to quantify the sensitivity of ambient air temperature to roof albedo under the hot and stagnant conditions associated with Guangzhou's heat waves. We compare the results of the regressions to show how much more variance in temperature change can be explained with these additional key meteorological properties.

$$\Delta T_{\text{cool}-\text{control}} = a_0 + a_1 \times T_{\text{control}} \quad \text{(Eq. 1)}$$

$$\Delta T_{\text{cool}-\text{control}} = a_0 + a_1 \times T_{\text{control}} + a_2 \times V_{\text{control}} \quad \text{(Eq. 2)}$$

$$\Delta T_{\text{cool}-\text{control}} = a_0 + a_1 \times T_{\text{control}} + a_2 \times V_{\text{control}} + a_3 \times H_{\text{control}} \quad \text{(Eq. 3)}$$

T and *H* are the episode average simulated 2-meter air temperature (° C) and 2-meter humidity (g water vapor per kg air), respectively, from 10:00 – 18:00 LST over the greater Guangzhou urban area (see the outline in Figure 1b). *V* is a measure of the ventilation of Guangzhou, calculated as the average mass air flow (Gtonnes air per hour) across the boundary and into the greater Guangzhou urban area from 10:00 – 18:00 LST for each episode. Note we did not calculate net air flow; we simply calculated the mass air flow only where and when the flow was directed into the city volume either horizontally or downwards into the first layer within the urban boundary. The horizontal boundary of the city volume was defined as the border shown in Figure 1b. The height of the city volume was defined as simply the first model layer. In the supplemental material we report alternate regression results where ventilation into the city was calculated based on the boundary layer height as opposed to simply the first model layer. The subtext "control" indicates the value was calculated based on a control simulation. $\Delta T_{\text{cool}-\text{control}}$ was calculated as the difference between average 2-meter temperatures in the cool scenario and the control scenario; thus, a negative value of $\Delta T_{\mathrm{cool-control}}$ indicates that the enhancement of urban albedo lead to a cooling of average air temperature across Guangzhou. We also note that adding the additional variable of solar insolation to Eq. 3 did not materially increase the amount of variance explained by the regression and thus we chose to exclude solar insolation from Eq. 3.

3 Results and discussion

3.1 Comparison of the control scenario simulations to observations

We compared control scenario simulated 2-meter air temperature to available corresponding observations from NOAA Global Summary of the Day (GSOD) data.54 Available temperature observations in the GSOD data include daily mean, maximum and minimum, but not hourly temperature recordings. We found all available GSOD observations close to the greater urban area of Guangzhou as defined as within the latitude-longitude box (22.46, 113.05) to (23.24,114.22). Across most episodes, only three GSOD observation locations were found within this location, two in the southern portion of the urban region and one just north of the urban region. To compare these point observations to modeled output, we averaged the observations across both time and space to yield one observed mean, maximum and minimum value per episode. We compared these averaged observations to the corresponding modeled values developed by selecting only grid cells within which we found GSOD observations. The comparison of modeled and observed values averaged over each episode is analogous to how we report results in this paper: that is, we also present result values as an average value over each episode.

a)

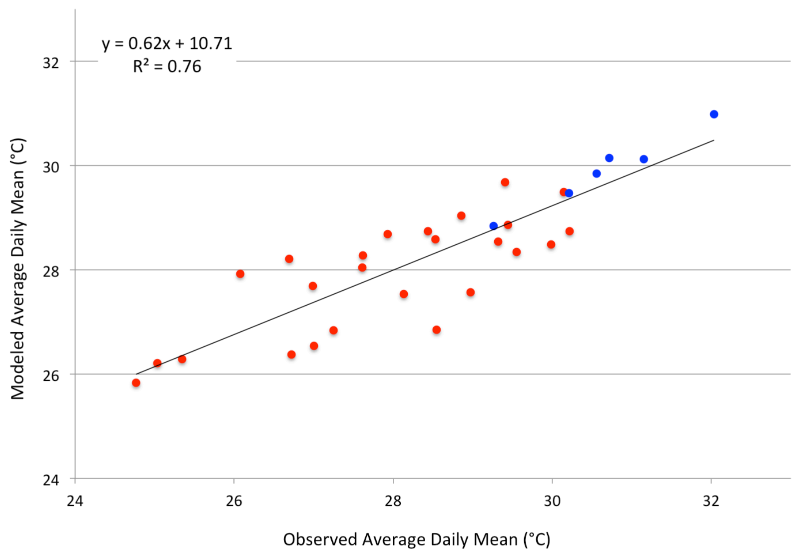

y = 0.62x + 10.71
R² = 0.76
Modeled Average Daily Mean (°C)
Observed Average Daily Mean (°C)

b)

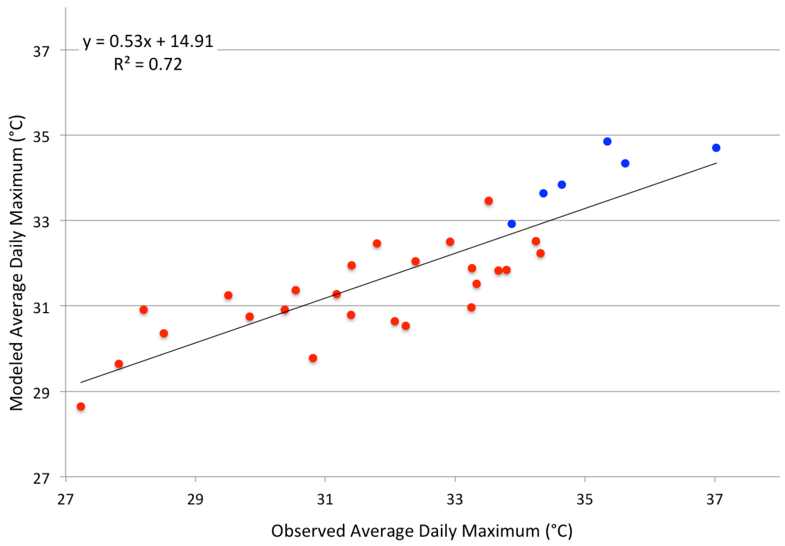

y = 0.53x + 14.91
R² = 0.72
Modeled Average Daily Maximum (°C)
Observed Average Daily Maximum (°C)

c)

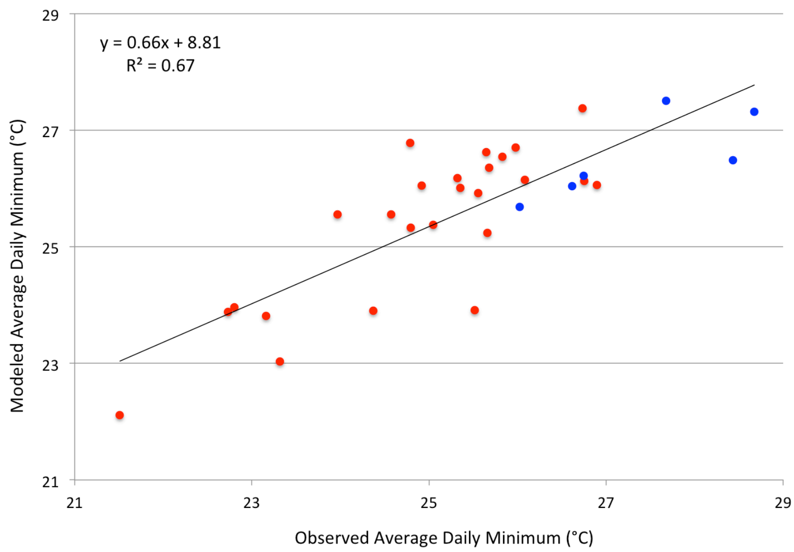

y = 0.66x + 8.81
R² = 0.67
Modeled Average Daily Minimum (°C)
Observed Average Daily Minimum (°C)

Figure 2. Comparison of modeled and observed episode averages of (a) mean, (b) daily maximum, and (c) daily minimum 2-meter air temperatures.

The model can explain 76%, 72%, and 67% of the variation (calculated as the coefficient of determination) in episode average mean, average daily maximum, and average daily minimum temperatures, respectively (see Figure 2). The mean bias for the mean, maximum and minimum values is -0.18 °C, -0.39 °C, and 0.21 °C, respectively. The mean error for the mean, maximum and minimum values is 0.82 °C, -1.24 °C, and 0.80 °C, respectively. The previous statistics are taken across all episodes. Isolating the six heat wave events, we find mean bias for the mean, maximum and minimum values to be -0.75 °C, -1.09 °C, and -0.82 °C, respectively. The mean error values are identical in magnitude to the mean bias values, but positive. Compared to the mean biases across the full set of episodes, the biases for the heat wave episodes are larger and all negative, indicating the model is not able to fully capture the temperature increases associated with the heat waves. However, the model can still explain much of the variation across the heat wave episodes, as the coefficient of determination calculated across the six episodes is equal to 0.97, 0.69, and 0.59 for the episode average mean, maximum, and minimum temperatures, respectively.

3.2 Simulated cool roof air temperature effects during heat waves and average summer conditions

Maps of mean 2-meter air temperatures and differences between the control and cool scenarios for the hours 10:00 – 18:00 LST are shown in Figure 3. The left column (Figure 3a-c) shows mean results of the normal summer episodes while the right column (Figure 3d-f) shows mean results from the heat-wave episodes. The greater urban area of Guangzhou is outlined in the center of each figure. A midday urban heat island effect can be clearly seen in Figure 3a. Figure 3b indicates that the simulated increase to roof albedo reduces the difference in average temperatures between urban Guangzhou and the surrounding area. High region-wide temperatures with peak temperatures centered in the urban area of Guangzhou can be seen in Figure 3d. Figures 3c and 3f show the simulated mean reduction to temperature with roof-albedo-increase under the normal episodes and heat-wave episodes, respectively.

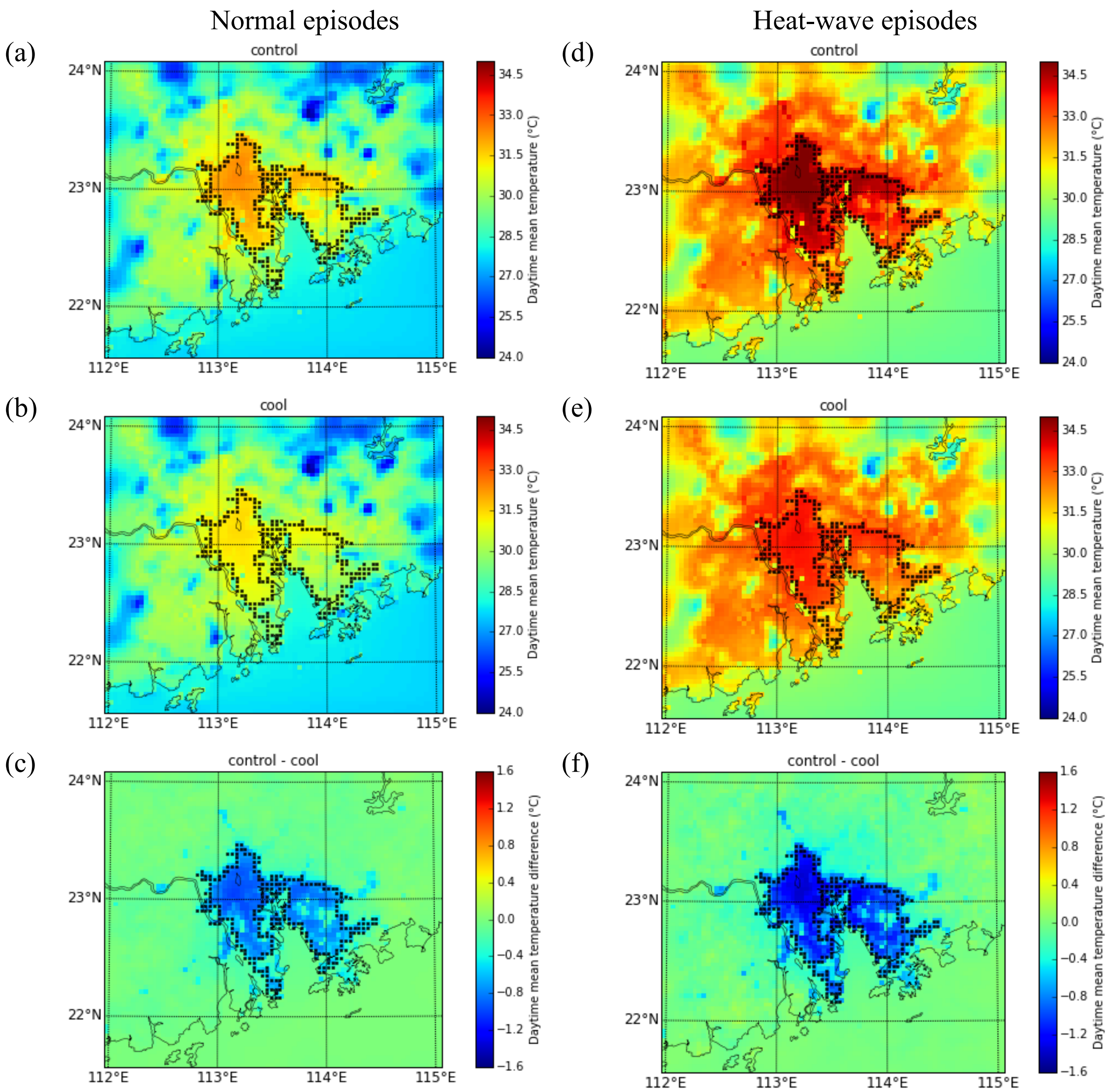

Figure 3. Mean temperature (a,b,d,e) and mean temperature change (c, f), 10:00 – 18:00 LST. Left column shows normal weeks, right column shows heat-wave events. The dotted line bounds the greater urban area of Guangzhou.

We found the cool simulations had reduced urban heat island intensity compared to the control simulations. To quantify this effect we define a heat island effect for each urban grid cell (536 cells) as the difference in temperature between that cell and the temperature averaged over all non-urban land based cells outside the greater Guangzhou urban area and located at an elevation under 200 meters (see Figure 1b for a map of the regions meeting these conditions). We averaged the temperatures average from 10:00 – 18:00 LST across all episodes (normal and heat-wave separately).

Under both the normal and heat-wave episodes, the cool simulations exhibit lower average urban temperatures and reduce the maximum heat island effect by roughly 1.0 °C. This can be seen in Figures 4a and b, which show histograms of the heat island effect during normal and heat-wave episodes. The larger cooling effect simulated during heat-wave episodes can be seen in Figure 4c, which shows a distribution of the temperature differences between the cool and control scenarios across the urban area of Guangzhou for both normal and heat-wave episodes.

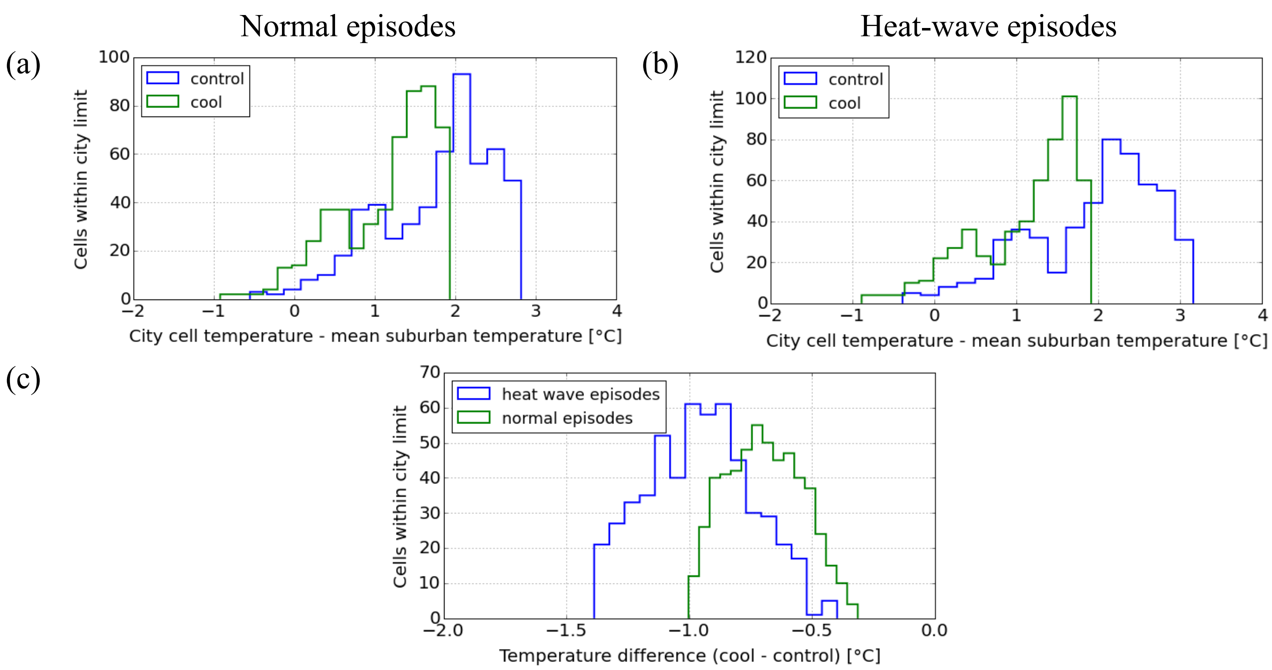

Figure 4. Panels (a) and (b) show the distribution of the heat island effect in the greater Guangzhou urban area during normal episodes and heat-wave episodes, respectively. Panel (c) shows the difference in temperature between the cool and control scenarios for normal and heat-wave episodes.

Examining the diurnal cycle of the mean differences in 2-meter temperature between the control and cool scenarios (calculated as the average temperatures across all grid cells within the greater Guangzhou urban area) we see that temperature reductions peak midday at 0.8 °C and 1.2 °C for the normal and heat-wave episodes, respectively (see Figure 5). We note the simulated cool roof effect on air temperatures at night is negligible with temperature changes averaging only -0.06 °C from 22:00 – 6:00 LST during normal episodes. Detailed data related to Figure 5 can be found in Tables S1 and S2.

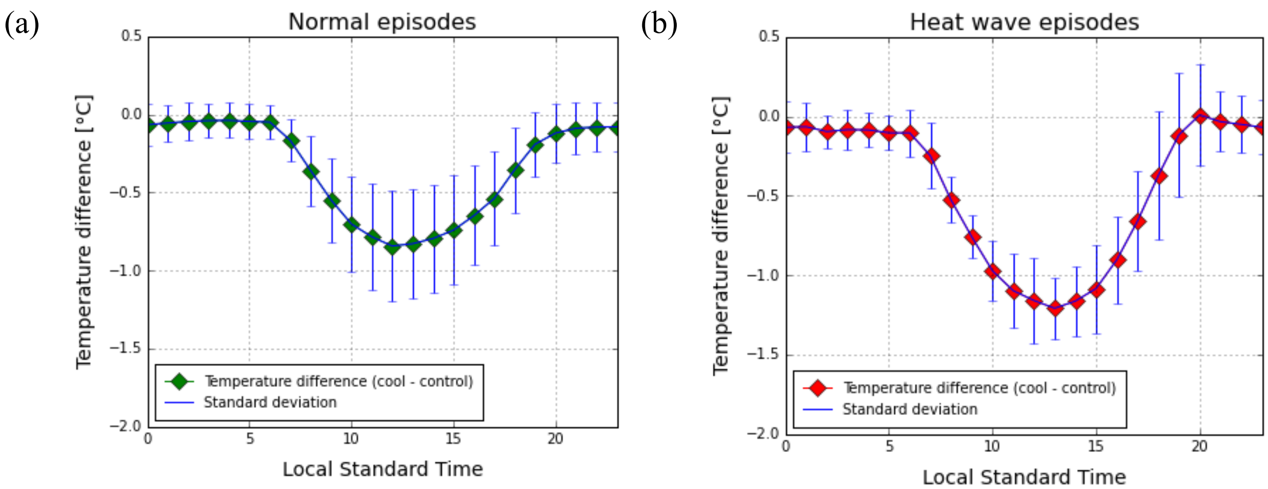

Figure 5. Diurnal cycle of mean temperature difference (± 1 standard deviation) between baseline and cool scenarios for (a) normal episodes and (b) heat-wave episodes.

3.3 Sensitivity of cool roof air temperature effects to meteorological conditions

We saw in Figures 3, 4 and 5 that average temperature reductions were greater during the heat-wave episodes. Here we investigate how the sensitivity of urban air temperature to roof albedo might vary under different meteorological conditions. Figure 6 shows a scatter plot of mean temperature reductions versus mean temperature of the control scenario, averaged across the greater Guangzhou urban area over the hours 10:00 – 18:00 LST. Following Equation 1 from section 3.2, we have regressed the data in Figure 6 finding a_0 = 1.42 and a_1 = -0.068 and a coefficient of determination (R^2) of 0.59.

We can explain more of the variance across these episodes by including other independent variables from the control scenario such as ventilation and humidity (see section 3.2 for details). Based on the full set of episodes (normal and heat-wave) we find coefficients a_0, a_1, and a_2 for Equation 2 of 1.125, -0.062 and 0.129, respectively, and coefficients a_0, a_1, a_2, and a_3 for Equation 3 of 1.084, -0.086, 0.120, and 0.046, respectively. Here, a_1, a_2, and a_3 are associated with temperature, ventilation and humidity, respectively. We find that by including these three meteorological properties we can account for greater than three fourths of the variance ($R^2 = 0.77$) in temperature response to albedo increase. By including ventilation in addition to temperature (compare Equation 2 to Equation 1) we are able to reduce the root-mean-square errors (RMSE) of the heat wave episodes but not the normal episodes. By including all three variables (Equation 3 compared to 1), we were able to reduce root-mean-square errors across both normal and heat-wave episodes. See Table 2 for the above results, and see Tables S3 and S4 for the results based on the ventilation into the full boundary layer, as discussed in Section 3.2.

This solution quantifies how increased ventilation and humidity attenuate the cool roof temperature effects. On average, compared to normal episodes, heat-wave episodes in Guangzhou were hotter (34.1 °C vs. 31.4°C) and had much lower midday ventilation (0.6 Gt/h vs. 0.9 Gt/h, a 33% decrease) but only slightly higher midday humidity (18.0 g/kg vs. 17.8 g/kg, a 1.2% increase). Running these average conditions through Equation 3, we find that cool roofs provide 0.26° C more cooling during heat waves compared to normal conditions, of which 0.23, 0.04 and −0.01 °C of cooling is associated with temperature, ventilation, and humidity differences, respectively. Thus, while the inclusion of ventilation and humidity can help explain some of the variation in cooling effects between heat-wave and normal episodes, the majority of the effect is associated with temperature differences.

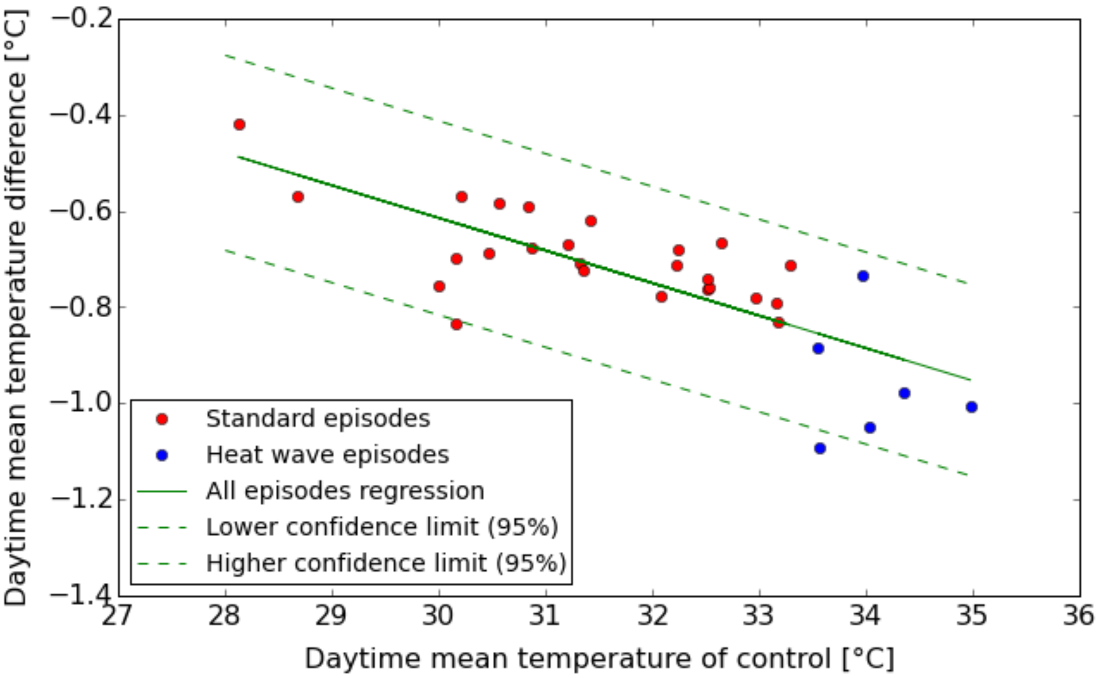

Figure 6. Mean (10:00 – 18:00 LST) temperature vs. mean temperature difference for normal and heat-wave episodes.

Table 2. Root-mean-square errors of ΔT calculated across normal, heat-wave and all episodes.

Linear regression	Root-mean-square error (° C) Normal episodes	Heat-wave episodes	All episodes	All episode coefficient of determination (R^2)
Eq. 1	0.077	0.138	0.092	0.59
Eq. 2	0.078	0.122	0.088	0.60
Eq. 3	0.055	0.098	0.065	0.77

3.4 Research and policy implications

We have shown through meteorological simulations that a policy of enhancing roof albedo in Guangzhou could reduce average midday summer temperatures by 0.8 °C. Furthermore those temperature reductions could be larger during the hot and stagnant conditions of heat waves in Guangzhou reaching 1.2 °C. The increased air temperature sensitivity to urban roof albedo during heat waves is important since heat waves can pose significant public health problems and electricity grids are typically under the most stress during heat waves. Our results highlight the need to evaluate cool roof meteorological effects under both average conditions as well as during heat waves in order to fully characterize potential urban cooling benefits. We note, however, these results are based on a scenario assuming the upper limit of feasible roof albedo enhancement. Given the challenge of changing the average roof albedo across an entire city, future modeling efforts might assist policy design by describing the minimum urban albedo change, in city area and in magnitude, required to provide measureable local benefits. Such efforts might also support a localized experiment that could help verify these simulations.

Acknowledgments

The authors would like to express their thanks for financial support from the US-China Clean Energy Research Center – Building Energy Efficiency and support from the Strategic Priority Research Program of the Chinese Academy of Sciences (XDA05110200) and the National Natural Science Foundation of China (Grant No. 41305093). The study was further supported by the Assistant Secretary for Energy Efficiency and Renewable Energy, Office of Building Technology, State, and Community Programs, of the U.S. Department of Energy under Contract No. DE-AC02-05CH11231. This research used resources of the National Energy Research Scientific Computing Center, a DOE Office of Science User Facility supported by the Office of Science of the U.S. Department of Energy under Contract No. DE-AC02-05CH11231.

Conflict of Interest Disclosure

The authors declare no competing financial interest.

Supporting Information

Supporting information includes tables of the average and standard deviation of temperature reductions by hour and simulation period. This material is available free of charge via the Internet at http://pubs.acs.org.

References:

1 Parker, D.S.; Barkaszi, S. F. Roof solar reflectance and cooling energy use: field research results from Florida. *Energy and Buildings*. **1997**, *25*, 105-115.

2 Akbari, H.; Konopacki, S.; Pomerantz, M. Cooling energy savings potential ofreflective roofs for residential and commercial buildings in the United States. *Energy.* **1999,** *24* (5), 391–407.

3 Levinson, R.; Akbari, H.; Konopacki, S.; Bretz, S. Inclusion of cool roofs in nonresidential Title 24 prescriptive requirements. *Energy Policy* **2005**, *33*, 151–170.

4 Levinson, R.; Akbari, H.; Potential benefits of cool roofs on commercial buildings: conserving energy, saving money, and reducing emission of greenhouse gases and air pollutants. *Energy Efficiency*. **2010**. *3* (1), 53-109.

5 Rosenfeld, A. H.; Akbari, H.; Romm, J. J.; Pomerantz, M. Cool communities: strategies for heat island mitigation and smog reduction. *Energy Build*. **1998**, *28*, 51–62.

6 Campra, P.; Garcia, M.; Canton, Y.; Palacios-Orueta, A. Surface temperature cooling trends and negative radiative forcing due to land use change toward greenhouse farming in southeastern Spain. *Journal of Geophysical Research.* **2008**, *113*, D18109. doi:10.1029/2008JD009912.

7 Zhou, Y.; Shepherd J. M. Atlanta's urban heat island under extreme heat conditions and potential mitigation strategies. *Natural Hazards.* **2009**, *52*, 639-668. DOI 10.1007/s11069-009-9406-z.

8 Millstein D.; Menon S. Regional climate consequences of large-scale cool roof and photovoltaic array deployment. *Environ. Res. Lett.*, **2011**. *6*, doi:10.1088/1748-9326/6/3/034001.

9 Campra P.; Millstein, D. “Mesoscale Climatic Simulation of Surface Air Temperature Cooling by Highly Reflective Greenhouses in SE Spain.” *Environ. Sci. Technol.* **2013,** 47 (21), 12284–12290.

10 Santamouris, M. Cooling the cities - A review of reflective and green roof mitigation technologies to fight heat island and improve comfort in urban environments. *Solar Energy*. **2014,** *103*, 682-703.

11 Millennium Ecosystem Assessment, *Ecosystems and Human Well-being: Synthesis*. Island Press, Washington, DC. 2005.

12 Akbari, H.; Menon, S.; Kosenfeld, A. Global cooling: increasing world-wide urban albedos to offset CO2. *Climatic Change.* **2009**, *94*, 275-286.

13 Menon, S.; Akbari, H.; Mahanama, S.; Sednev, I.; Levinson, R. Radiative forcing and temperature response to changes in urban albedos and associated CO2 offsets. *Environ. Res. Lett.* **2010**, *5*, doi:10.1088/1748-9326/5/1/014005.

14 Oleson,K. W.; Bonan, G. B.; Feddema J. Effects of white roofs on urban temperature in a global climate model. *Geophys. Res. Lett.* **2010**, *37*, L03701, doi:10.1029/2009GL042194.

15 Akbari, H.; Matthews, H. D.; Seto, D. The long-term effect of increasing the albedo of urban areas. *Environ. Res. Lett.* **2012**, *7*, doi:10.1088/1748-9326/7/2/024004.

16 Jacobson, M.Z.; Ten Hoeve, J. E. Effects of urban surfaces and white roofs on global and regional climate. *Journal of Climate*, **2012**, 25 (3) 1028-1044.

17 Georgescu, M.; Morefield, P. E.; Dierwagen, B. G.; Weaver, C.P.; Urban adaptation can roll back warming of emerging megapolitan regions. *Proceedings of the National Academy of Sciences*, **2014**. 111 (8), 2909-2914.

18 Akbari, H.; Levinson, R. M. Evolution of cool roof standards in the United States. *Advances in Building Energy Research.* **2008,** *2* (1), 1-32.

19 Gilbert, H.; Mandel, B, H.; Levinson, R. Keeping California cool: Recent cool community developments. *Energy and Buildings*. **2015**, *Corrected Proof, In press*. http://dx.doi.org/10.1016/j.enbuild.2015.06.023.

20 Gao, Y.; Xu, J.; Yang, S.; Tang, X.; Zhou, Q.; Ge, J.; Xu, T.; Levinson, R. Cool roofs in China: Policy review, building simulations, and proof-of-concept experiments. *Energy Policy*. **2014**, *74*, 190–214.

21 *U.S.-China Clean Energy Research Center Building Energy Efficiency (CERC-BEE) Consortium* Website; http://cercbee.lbl.gov.

22 Wang, M.; Yan, X.; Liu, J.; Zhang, X. The contribution of urbanization to recent extreme heat events and a mitigation strategy in the Beijing-Tianjin-Hebei metropolitan area. *Thero. Appl. Climatol.* **2013**, *114*, 407-416.

23 Ma H.; Shao H.; Song J. Modeling the relative roles of the foehn wind and urban expansion in the 2002 Beijing heat wave and possible mitigation by high reflective roofs. *Meteorol. Atmos. Phys.* **2014**, *123*, 105-114.

24 Li, D.; Sun, T.; Liu, M.; Yang, L.; Wang, L.; Gao, Z. Contrasting responses of urban and rural surface energy budgets to heat waves explain synergies between urban heat islands and heat waves. *Environ. Res. Lett.* **2015**, *10*, 054009. doi:10.1088/1748-9326/10/5/054009.

25 Luber G.; McGeehin M. Climate Change and Extreme Heat Events, *American Journal of Preventive Medicine*, 2008, *35* (5), 429-435. doi:10.1016/j.amepre.2008.08.021.

26 Poumade`re, M.; Mays, C.; Le Mer, S.; Blong, R.; The 2003 Heat Wave in France: Dangerous Climate Change Here and Now. *Risk Analysis*. **2005**, *25* (6), 1483-1494.

27 Miller, N. L.; Hayhoe, K.; Jin, J.; Auffhammer, M. Climate, Extreme Heat, and Electricity Demand in California. *Journal of Applied Meteorology and Climatology*. **2008**, *47*, 1834-1844. DOI: 10.1175/2007JAMC1480.1.

28 Yang, J.; Liu, H. Z.; Ou, C. Q.; Lin, G. Z.; Ding, Y.; Zhou, Q.; Shen, J. C.; Chen, P. Y. Impact of heat wave in 2005 on mortality in Guangzhou, China. *Biomed. Environ. Sci.* **2013**, *26*, 647-654.

29 Lu, S.; Ye, M. The research on relationship between outer circulation of tropical cyclones and high temperature weather in Guangzhou. *J. Tropic. Meteor.* **2006**, *22* (5), 461-465. (in Chinese)

30 Taha H. Meteorological, air-quality, and emission-equivalence impacts of urban heat island control in California. *Sustainable Cities and Society*. **2015**, *19,* 207-221. doi:10.1016/j.scs.2015.03.009.

31 Mihalakakou, G.; Flocas, H. A.; Santamouris, M.; Helmis C. G. Application of Neural Networks to the Simulation of the Heat Island over Athens, Greece, Using Synoptic Types as a Predictor. *Journal of Applied Meteorology and Climatology*, **2002,** *41* (5), 519–527. doi: http://dx.doi.org/10.1175/1520-0450(2002)041<0519:AONNTT>2.0.CO;2.

32 Zhao, L.; Lee, X.; Smith, R. B.; Oleson, K. Strong contributions of local background climate to urban heat islands. *Nature.* **2014**, *511*, 216–219. doi:10.1038/nature13462.

33 Georgescu, M. Challenges associated with adaptation to future urban expansion. *Journal of Climate*. **2015**. 28 (7), 2544-2563.

34 Skamarock, W. *et al.* A description of the advanced research WRF version 3. NCAR Technical Note, **2008**, NCAR/TN-475+STR.

35 Zhang, Q.; Huang, J.; Lang, S. Development of typical year weather data for Chinese location. *ASHRAE Trans*. **2002**, *108* (2), 1063–1075.

36 Reynolds, R. W.; Smith, T. M.; Liu, C.; Chelton, D. B.; Casey, K. S.; Schlax, M. G. Daily high-resolution-blended analyses for sea surface temperature. *J. Climate*. **2007**, *20*, 5473-5496.

37 Csiszar, I.; Gutman, G. Mapping global land surface albedo from NOAA AVHRR. *J. Geophys. Res.* **1999**, *104*, 5215-6228.

38 Kusaka, H.; Kondo, H.; Kikegawa, Y.; Kimura, F. A simple single-layer urban canopy model for atmospheric models: Comparison with multi-layer and slab models. *Boundary-Layer Meteorology,* **2001**, *101* (3), 329-358.

39 Chen, F.; Zhang, Y. On the coupling strength between the land surface and the atmosphere: from viewpoint of surface exchange coefficients. *Geophys. Res. Lett.* **2009**, *36*, L10404, doi:10.1029/2009GL037980.

40 Miao, S.; Chen, F. Formation of horizontal convective rolls in urban areas. *Atmos. Res.* **2008**, *89*, 298-304.

41 Li, D.; Bou-Zeid, E.; Barlage, M.; Chen, F.; Smith, J. Development and evaluation of a mosaic approach in the WRF-Noah framework. *J. Geophys. Res.* **2014**, *118*, 918-935.

42 Jimenez, P. S.; Dudhia, J.; González-Rouco, J. F.; Navarro, J.; Montávez, J. P.; García-Bustamante E. A revised scheme for the WRF surface layer formulation. *Mon. Wea. Rev.* **2012**, *140*, 898-918.

43 Hong, S.; Noh, Y.; Dudhia, J A new vertical diffusion package with an explicit treatment of entrainment processes. *Mon. Wea. Rev.* **2006**, *134*, 2318-2341.

44 Iacono, M. J.; Delamere, J. S.; Mlawer, E. J.; Shephard, M. W.; Clough, S. A.; Collins W. D. Radiative forcing by long-lived greenhouse gases: Calculations with the AER radiative transfer models. *J. Geophys. Res.* **2008**, *113*, D13103, doi:10.1029/2008JD009944.

45 Chen, S.; Sun, W. A one dimensional, time dependent cloud model. *J. Meteor. Soc. Japan*. **2002**, *1860*, 99-1.

46 Grell, G.; Freitas, S. A scale and aerosol aware stochastic convective parameterization for weather and air quality modeling. *Atmos. Chem. Phys. Discuss.* **2013**, *13*, 23845-23893.

47 *Cool Roof Rating Council Rated Products Directory* Website; http://coolroofs.org.

48 Sleiman, M.; Ban-Weiss, G.; Gilbert, H. E.; François, D.; Berdahl, P.; Kirchstetter, T. W.; Destaillats, H.; Levinson, R. M. Soiling of building envelope surfaces and its effect on solar reflectance—Part I: Analysis of roofing product databases. *Solar Energy Materials and Solar Cells.* **2011**, *95* (12), 3385-3399.

49 Liang, F.; Zhang, L.; Xu, X. The relationship between hot days and typhoon in Guangzhou. *Tropical Geography*, **1988**, *8* (4), 345-354. (in Chinese).

50 Ji, Z.; Lin, G.; Li, X.; Xiong, Y. High temperature anomalies in Guangzhou in summer 2003 and its climatic background. *J. Tropic. Meteor.* **2005**, *21* (2), 207-216. (in Chinese).

51 Meng, W.; Zhang, Y.; Li, J.; Lin, W.; Dai, G.; Li, H. Application of WRF/UCM in the simulation of a heat wave event and urban heat island around Guangzhou city. *J. Tropic. Meteor.* **2010**, *26* (3), 273-282. (in Chinese).

52 Meng, W.; Zhang, Y.; Li, J.; Lin, W.; Dai, G.; Li, H. Application of WRF/UCM in the simulation of a heat wave event and urban heat island around Guangzhou city. *J. Tropic. Meteor.* **2011**, *17* (3), 257-267. (in English).

53 Huang, Y.; Yan, J.; Meng, W.; Wan, Q. Improvement of summer high temperature forecasting in Guangzhou during the typhoon period using a BDA scheme. *Acta Meteorologica Sinica*, **2010**, *68* (1), 102-113. (in Chinese).

54 National Climatic Data Center, NESDIS, NOAA, U.S. Department of Commerce: Global Surface Summary of the Day – GSOD, Asheville, NC. Accessed 2014. http://gcmd.gsfc.nasa.gov/records/GCMD_gov.noaa.ncdc.C00516.html.